THE JOURNAL OF BIOLOGICAL CHEMISTRY VOL. 283, NO. 16, pp. 10716–10726, April 18, 2008

Filamentous Actin Regulates Insulin Exocytosis through Direct Interaction with Syntaxin 4*

Received for publication, December 4, 2007, and in revised form, February 13, 2008 Published, JBC Papers in Press, February 19, 2008, DOI 10.1074/jbc.M709876200

Jenna L. Jewell[‡1], **Wei Luo**[§1], **Eunjin Oh**[‡], **Zhanxiang Wang**[‡], **and Debbie C. Thurmond**[‡2]

From the [‡]*Department of Biochemistry and Molecular Biology, Center for Diabetes Research, Indiana University School of Medicine, Indianapolis, Indiana 46202 and* [§]*GenScript Corporation, Piscataway, New Jersey 08854*

Glucose-induced insulin exocytosis is coupled to associations between F-actin and SNARE proteins, although the nature and function of these interactions remains unknown. Toward this end we show here that both Syntaxin 1A and Syntaxin 4 associated with F-actin in MIN6 cells and that each interaction was rapidly and transiently diminished by stimulation of cells with D-glucose. Of the two isoforms, only Syntaxin 4 was capable of interacting directly with F-actin in an *in vitro* sedimentation assay, conferred by the N-terminal 39–112 residues of Syntaxin 4. The 39–112 fragment was capable of selective competitive inhibitory action, disrupting endogenous F-actin-Syntaxin 4 binding in MIN6 cells. Disruption of F-actin-Syntaxin 4 binding correlated with enhanced glucose-stimulated insulin secretion, mediated by increased granule accumulation at the plasma membrane and increased Syntaxin 4 accessibility under basal conditions. However, no increase in basal level Syntaxin 4-VAMP2 association occurred with either latrunculin treatment or expression of the 39–112 fragment. Taken together, these data disclose a new underlying mechanism by which F-actin negatively regulates exocytosis via binding and blocking Syntaxin 4 accessibility, but they also reveal the existence of additional signals and/or steps required to trigger the subsequent docking and fusion steps of exocytosis.

Insulin granules are exocytosed in two distinct phases. First-phase insulin granule release involves the rapid fusion of a small pool of granules that are already present at the plasma membrane under basal conditions, termed the readily releasable pool, and these granules will discharge their cargo in response to nutrient and also non-nutrient secretagogues (1–4). In contrast, second-phase secretion is evoked only in response to nutrients and involves additional steps such as the mobilization of intracellular storage granules, targeting of granules to SNARE[3] sites for docking and fusion steps of exocytosis and insulin release. Remarkably, although the actin cytoskeleton has been considered to play a principle regulatory role in glucose-stimulated insulin secretion since 1968 (5, 6), the lack of mechanistic data has impeded the inclusion of cytoskeletal input into models detailing the regulation of biphasic insulin release.

F-actin was originally shown to function as a "cell web" in islet beta cells (7–10). This notion was consistent with observations from other cell types and led to the concept that cytoskeletal disruption serves as a mechanism to clear away the F-actin barrier and permit access of granules to the plasma membrane (11–14). However this model did not suffice to explain why insulin granule transport still requires F-actin as a motive force (9, 15), nor did it explain why F-actin is both increased and decreased by glucose (16–19). Distinct from neurotransmitter exocytosis or GLUT4 translocation events that are impacted by F-actin, insulin release occurs over a long time period and in discrete phases, requiring the readily releasable pool of granules at the plasma membrane to be refilled from the more intracellular storage pool in a carefully metered manner. More recently, glucose-induced F-actin remodeling in beta cells has been visualized by dynamic changes in cortical F-actin (20–23). No changes in the F/G-actin ratio were detected, indicating that the F-actin was being remodeled and reorganized as opposed to a general loss of cellular F-actin content in response to glucose. Remodeling occurred specifically in response to D-glucose, and not L-glucose or KCl stimulation, and was coupled to SNARE protein-mediated exocytosis.

Insulin granule exocytosis requires two syntaxin isoforms: Syntaxin 1A and Syntaxin 4. Syntaxin 1A null mouse islets show significantly fewer predocked granules, which support first-phase insulin release in response to calcium influx, although second-phase secretion is normal (24). Syntaxin 4 heterozygous knock-out mouse islets show decreased first-phase secretion and also a slight decrease in second-phase secretion (25). In addition, Syntaxin 4 overexpressing transgenic mouse islets have enhanced second-phase secretion (25). Other cell systems that utilize multiple syntaxins show partitioning of interactions and localization to particular membrane compartments to achieve differential modes of vesicle targeting and fusion (26, 27). Characterization of unique features of Syntaxin 1A and Syntaxin 4 will be required before a mechanistic understanding

* This work was supported by Grants DK-067912 and DK-76614 from the National Institutes of Health and 1-03-CD-10 from the American Diabetes Association (to D. C. T.) and Postdoctoral Fellowship 0720042Z from the American Heart Association (to E. O.). The costs of publication of this article were defrayed in part by the payment of page charges. This article must therefore be hereby marked "*advertisement*" in accordance with 18 U.S.C. Section 1734 solely to indicate this fact.

[1] These authors contributed equally.

[2] To whom correspondence should be addressed: 635 Barnhill Dr., MS4053, Dept. of Biochemistry and Molecular Biology, Indianapolis, IN 46202. Tel.: 317-274-1551; Fax: 317-274-4686; E-mail: dthurmon@iupui.edu.

[3] The abbreviations used are: SNARE, soluble *N*-ethylmaleimide-sensitive factor attachment protein receptor; BSA, bovine serum albumin; GFP, green fluorescent protein; EGFP, enhanced green fluorescence protein; MKRBB, modified Krebs-Ringer bicarbonate buffer; PM, plasma membrane; SG, storage granule; Cyt, cytosol; PVDF, polyvinylidene difluoride; GST, glutathione *S*-transferase.

of their different roles in biphasic insulin release can be discerned.

We have previously demonstrated that, in rodent islet beta cells, glucose-induced insulin exocytosis is coupled to the interaction of F-actin with t-SNARE proteins (21). Here, we have demonstrated the relevance of this to human islet function and expanded upon the underlying mechanism by showing that F-actin bound directly to a novel motif in the N terminus of Syntaxin 4. We found that competitive inhibition of the direct association between F-actin-Syntaxin 4 increased unstimulated granule accumulation at the plasma membrane as well as Syntaxin 4 accessibility to VAMP2. Interestingly however, VAMP2 association with syntaxin was not increased upon release of F-actin binding from Syntaxin 4, suggesting the requirement for an additional stimulus-dependent/induced step that precedes the docking and fusion steps in exocytosis.

EXPERIMENTAL PROCEDURES

Materials—Rabbit polyclonal Syntaxin 4 and mouse monoclonal Syntaxin 1 antibodies were obtained from Chemicon (Temecula, CA) and Upstate Biotechnology (Lake Placid, NY), respectively. The mouse anti-insulin and rabbit anti-actin antibodies were obtained from Sigma. Rabbit anti-GFP antibody was acquired from Abcam (Cambridge, MA). Monoclonal anti-SNAP-25 and anti-GFP antibodies were purchased from BD Biosciences/Clontech. The mouse monoclonal anti-VAMP2 antibody and recombinant soluble Syntaxin 1A protein were obtained from Synaptic Systems (Gottingen, Germany). Latrunculin B was purchased from Calbiochem. Texas Red-conjugated secondary antibody and control mouse and rabbit IgG for immunoprecipitation were purchased from Jackson Immunoresearch Laboratories (West Grove, PA). Radioimmunoassay-grade bovine serum albumin and D-glucose were purchased from Sigma. The MIN6 cells were a gift from Dr. John Hutton (University of Colorado Health Sciences Center). Goat anti-mouse and anti-rabbit horseradish peroxidase secondary antibodies and TransFectin lipid reagent were acquired from Bio-Rad. ECL reagent was purchased from Amersham Biosciences. The human C-peptide and rat insulin radioimmunoassay kits were purchased from Linco Research Inc. (St. Charles, MO). The actin binding spin-down assay and F/G-actin quantitation kits were purchased from Cytoskeleton (Denver, CO).

Plasmids—pGEX-4T1-VAMP2-(1–94) was generated as described previously (28). The pGEX-4T1-Syntaxin 4-(1–193), -(1–112), and -(1–70) cDNA constructs were generated by subcloning PCR-generated rat Syntaxin 4 fragments into the SalI and XhoI sites of the pGEX-4T1 expression vector. The pGEX-4T1-Syntaxin 4-(1–273) and -(39–273) cDNA constructs were made by subcloning PCR-generated fragments into the EcoRI and XhoI sites of pGEX-4T1. The pEGFP-Syntaxin 4-(39–112) cDNA construct was generated by subcloning the PCR-generated Syntaxin 4 fragment engineered with 5′-EcoRI and 3′-XhoI sites into the 5′-EcoRI and 3′-SalI sites of the EGFP-C2 vector (Clontech). All constructs were verified by DNA sequencing.

Isolation, Culture, and Stimulation of Insulin Secretion of Mouse and Human Islets—Pancreatic mouse islets were isolated as previously described (29, 30). Briefly, pancreata from 8–12-week-old male mice were digested with collagenase and purified using a Ficoll density gradient. After isolation, islets were cultured overnight in CMRL-1066 medium. Fresh islets were handpicked into groups of 10, preincubated in Krebs-Ringer bicarbonate buffer (10 mM HEPES, pH 7.4, 134 mM NaCl, 5 mM $NaHCO_3$, 4.8 mM KCl, 1 mM $CaCl_2$, 1.2 mM $MgSO_4$, 1.2 mM KH_2PO_4) containing 2.8 mM glucose and 0.1% BSA for 1.5 h in the presence of 10 μM latrunculin or DMSO vehicle followed by stimulation with 20 mM glucose for 2 h. Medium was collected to measure insulin secretion, and islets were harvested in Nonidet P-40 lysis buffer to determine cellular insulin content by radioimmunoassay. Human islets isolated from two independent nondiabetic donors were obtained through the National Institutes of Health/ICR (islet cell resource) distribution program, and used in experiments identical in design to those described above with mouse islets.

Cell Culture, Transient Transfection, and Secretion Assays—MIN6 beta cells were cultured in Dulbecco's modified Eagle's medium (25 mM glucose) supplemented with 15% fetal bovine serum, 100 units/ml penicillin, 100 μg/ml streptomycin, 292 μg/ml L-glutamine, and 50 μM β-mercaptoethanol as described previously (31). MIN6 beta cells at ~60% confluence were transfected with 40 μg of plasmid DNA/10-cm^2 dish using TransFectin (Bio-Rad) to obtain ~30–50% transfection efficiency. After 48 h of incubation, cells were washed twice with and incubated for 2 h in freshly prepared modified Krebs-Ringer bicarbonate buffer (MKRBB: 5 mM KCl, 120 mM NaCl, 15 mM HEPES, pH 7.4, 24 mM $NaHCO_3$, 1 mM $MgCl_2$, 2 mM $CaCl_2$, and 1 mg/ml radioimmunoassay-grade BSA). Cells were stimulated with 20 mM glucose for the amount of time indicated in the figures after which the buffer was collected and microcentrifuged for 5 min at 4 °C to pellet cell debris, and insulin secreted into the buffer was quantitated using a rat insulin immunoassay kit (Linco Research). Cells were harvested in Nonidet P-40 lysis buffer (25 mM Tris, pH 7.4, 1% Nonidet P-40, 10% glycerol, 50 mM sodium fluoride, 10 mM sodium pyrophosphate, 137 mM NaCl, 1 mM sodium vanadate, 1 mM phenylmethylsulfonyl fluoride, 10 μg/ml aprotinin, 1 μg/ml pepstatin, 5 μg/ml leupeptin) containing 60 mM *n*-octylglucoside and lysed for 10 min at 4 °C, and lysates were cleared of insoluble material by microcentrifugation for 10 min at 4 °C for subsequent use in co-immunoprecipitation experiments. For measurement of human C-peptide release, MIN6 beta cells were transiently co-transfected with each plasmid plus human proinsulin cDNA (kind gift from Dr. Chris Newgard, Duke University). Forty-eight h after transfection, cells were preincubated for 2 h in MKRBB buffer and stimulated with 20 mM glucose for 1 h. MKRBB was collected for quantitation of human C-peptide released.

Immunofluorescence and Confocal Microscopy—MIN6 cells at 40% confluency plated onto glass coverslips were preincubated in MKRBB in the absence or presence of latrunculin (10 μM) or vehicle (Me_2SO) for 1–2 h followed by stimulation with 20 mM glucose for 5 min and then immediately fixed and permeabilized in 4% paraformaldehyde and 0.1% Triton X-100 for 10 min at 4 °C. Fixed cells were blocked in 1% BSA plus 5%

donkey serum for 1 h at room temperature followed by incubation with insulin antibody (1:100) for 1 h. MIN6 cells were then washed with phosphate-buffered saline (pH 7.4) and incubated with anti-mouse Texas Red secondary antibody for 1 h. All cells were washed again in phosphate-buffered saline, overlaid with Vectashield mounting medium, and mounted for confocal fluorescence microscopy using a Zeiss 510 confocal microscope. EGFP and insulin-Texas Red fluorescing cells were imaged using single-channel scanning using a ×100 objective.

Electron Microscopy—MIN6 beta cells were grown to ~80% confluence on Thermonox coverslips. Cells were washed twice with and incubated for 2 h in freshly prepared modified Krebs-Ringer bicarbonate buffer followed by the addition of either latrunculin B or Me_2SO vehicle for an additional 30 min. Cells were fixed in a 0.1 M cacodylate-buffered mixture of 2% glutaraldehyde and 2% paraformaldehyde for 30 min at room temperature followed by overnight incubation at 4 °C and then post-fixed in 1% OsO_4 in for 1 h. En bloc staining in 0.5% aqueous uranyl acetate was performed for 3 h followed by a 10-min water wash. Dehydration was done in the following sequence: 50% ethanol, 70% ethanol, 95% ethanol, and 100% ethanol each for 10 min. Infiltration entailed ethanol and resin in the order of 3:1 (1 h), 1:1 (overnight), 1:3 (1 h), and 100% resin (2–3 changes each 30 min). The Thermonox coverslips were inverted over a 1.5-ml centrifuge tube filled with resin and polymerized for 48 h at 60 °C. Thick (0.5–2.0 μm) and thin (60–100 nm) sections were cut using the microtome (Leica Ultracut). The thin sections were stained with uranyl acetate and lead citrate and viewed on the FEI Tecnai G2 Biotwin.

Subcellular Fractionation—Subcellular fractions of beta cells were isolated as described previously (28). Briefly, MIN6 beta cells at 80–90% confluence were harvested into 1 ml of homogenization buffer (20 mM Tris-HCl, pH 7.4, 0.5 mM EDTA, 0.5 mM EGTA, 250 mM sucrose, 1 mM dithiothreitol, and 1 mM sodium orthovanadate) containing protease inhibitors. Cells were disrupted by 10 strokes through a 27-gauge needle and homogenates centrifuged at 900 × *g* for 10 min. Postnuclear supernatants were centrifuged at 5,500 × *g* for 15 min, and the subsequent supernatant was centrifuged at 25,000 × *g* for 20 min to obtain the storage granule (SG) fraction in the pellet. The supernatant was further centrifuged at 100,000 × *g* for 1 h to obtain the cytosolic fraction (Cyt). Plasma membrane (PM) fractions were obtained by mixing the postnuclear pellet with 1 ml of buffer A (0.25 M sucrose, 1 mM $MgCl_2$, d 10 mM Tris-HCl, pH 7.4) and 2 volumes of buffer B (2 M sucrose, 1 mM $MgCl_2$, d 10 mM Tris-HCl, pH 7.4). The mixture was overlaid with Buffer A and centrifuged at 113,000 × *g* for 1 h to obtain an interface containing the plasma membrane fraction. The interface was collected and diluted to 2 ml with homogenization buffer for centrifugation at 6,000 × *g* for 10 min, and the resulting pellet was collected as the plasma membrane fraction. All pellets were resuspended in 1% Nonidet P-40 lysis buffer to ensure solubilization of membrane proteins.

Co-immunoprecipitation and Immunoblotting—MIN6 beta cell cleared detergent homogenates (2–3 mg) were combined with rabbit anti-Syntaxin 4 or mouse anti-Syntaxin 1 antibodies for 2 h at 4 °C followed by a second incubation with protein G Plus-agarose for 2 h. The resultant immunoprecipitates were subjected to 12% SDS-PAGE followed by transfer to PVDF membranes for immunoblotting. Membranes were blocked in 5% milk/TBS-Tween for 1 h at room temperature followed by immunoblotting (Syntaxin 1A, Syntaxin 4,and SNAP-25 antibodies were used at 1:1000; VAMP2 antibody was used at 1:5000). Proteins were visualized by enhanced chemiluminescence for quantitation using a Chemi-Doc gel documentation system (Bio-Rad).

Recombinant Proteins and Interaction Assays—GST-VAMP2-(1–94) fusion protein was expressed in *Escherichia coli* and purified by glutathione-agarose affinity chromatography as described (28). GST-VAMP2 was immobilized on Sepharose beads and incubated with cleared detergent lysates (~3 mg) prepared from unstimulated cells for 2 h at 4 °C. Following three washes with 1% Nonidet P-40 lysis buffer, proteins were eluted from the Sepharose beads and subjected to electrophoresis on 12% SDS-PAGE followed by transfer to PVDF membrane for immunoblotting with Syntaxin 4 antibody. For the F-actin spin-down assays, recombinant VAMP2 and Syntaxin 4 proteins were initially expressed and purified as GST fusion proteins after which the GST was removed by thrombin cleavage and remaining protein captured (Novagen kit). Syntaxin 1A protein was purchased from Synaptic Systems. Proteins were concentrated to ~20 μM and centrifuged at 150,000 × *g* for 1 h at 4 °C immediately prior to use of the resulting supernatant in an actin binding assay. Purified F-actin stocks (23 μM) were prepared according to manufacturer's instructions. Test proteins were incubated with F-actin stock in actin polymerization buffer at room temperature for 30 min. BSA and α-actinin control proteins provided by the manufacturer were used as negative and positive F-actin binding control proteins, respectively, in each experiment for validation of binding. All reactions were centrifuged at 150,000 × *g* for 1.5 h at 24 °C, and supernatants were removed into individually labeled new tubes on ice. Both the supernatants and the pellets were subjected to 12–18% SDS-PAGE followed by transfer to PVDF membranes for Coomassie staining or immunoblotting analyses.

Statistical Analysis—All data are expressed as mean ± S.E. Data were evaluated for statistical significance using Student's *t* test.

RESULTS

F-actin Function Is Conserved between Human and Rodent islet Beta Cells—We previously reported that treatment of rat islets with latrunculin B results in potentiation of glucose-stimulated insulin release (21). Latrunculin is a potent actin monomer-binding and sequestering agent that converts cellular F-actin to G-actin. To establish continuity of function among islet model systems, the impact of latrunculin upon secretion from mouse islets and human islets was evaluated. Similar to rat islets, isolated mouse islets showed a robust response to 2 h of glucose stimulation, which was further potentiated by latrunculin (Fig. 1*A*). Human islets were obtained from three independent nondiabetic human cadaver pancreases through the National Institutes of Health/ICR/ABCC (Administrative and Bioinformatics Coordinating Center) distribution program. Because of the fragility of these human islets following isolation

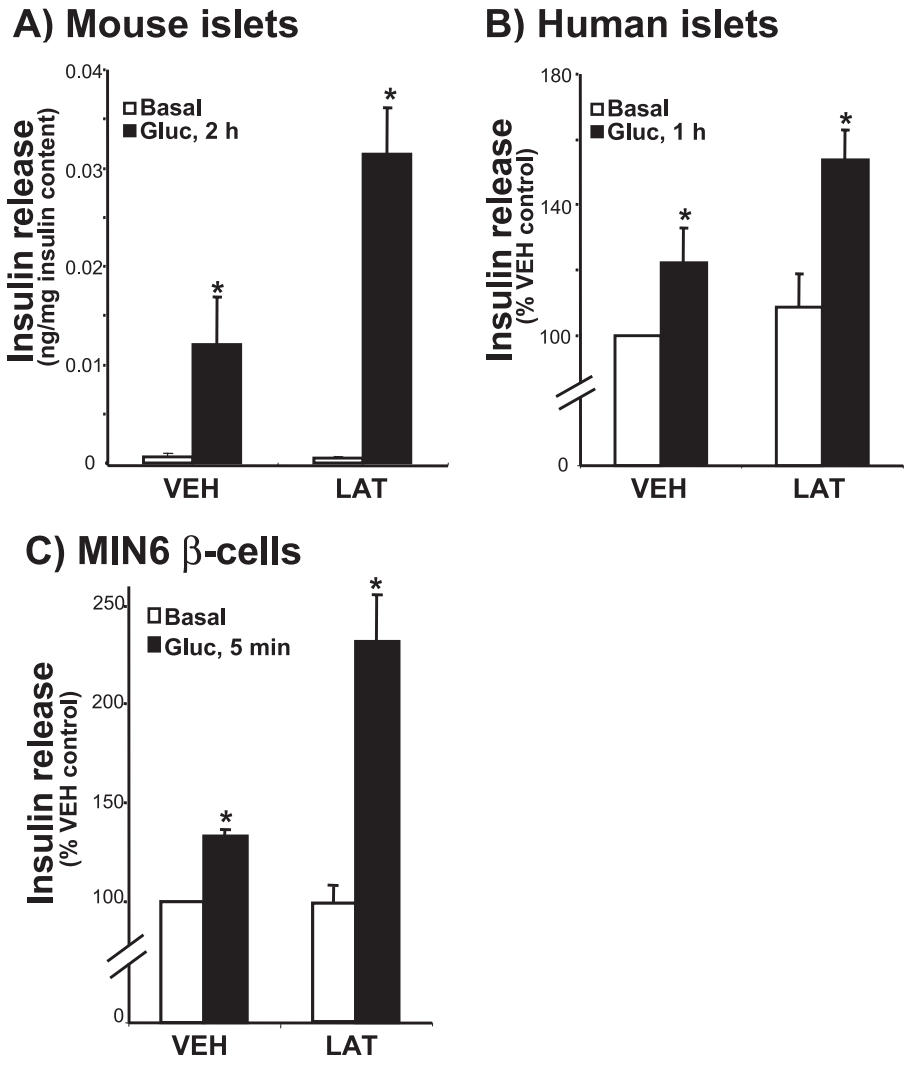

FIGURE 1. **Latrunculin potentiates insulin secretion in human islets: conservation of function with rodent islets and cultured beta cells.** *A*, mouse islets were handpicked for a 2-h preincubation in KRB with 2.8 mM glucose ± latrunculin (*LAT*; 10 μM) and then 2 h more under basal or stimulated conditions (20 mM glucose (*Gluc*)) with 10 islets/condition performed in duplicate. Three independent sets of mouse islets were combined; data are expressed as insulin secretion normalized to insulin content. *, $p < 0.05$, *versus* vehicle (*VEH*)-basal condition. *B*, human islets were isolated from cadaver pancreas at the ICR center and shipped for receipt within 48 h of isolation. Islets were allowed to recover for 3 h and then handpicked for preincubation for 1 h in KRB containing 2 mM glucose ± latrunculin (10 μM LAT) followed by 1 h of incubation under basal (2.8 mM glucose) or stimulated conditions (20 mM glucose). Data represent the average of three independent batches of human islets normalized for insulin content and expressed as percent vehicle-basal secretion set equal to 100% (*, $p < 0.05$, *versus* vehicle-basal condition). *C*, MIN6 cells were preincubated in glucose-free MKRBB containing vehicle or LAT for 2 h and then stimulated with 20 mM glucose for 5 min. Data represent the average of six independent sets of MIN6 cells normalized for protein content and expressed as percent vehicle-basal secretion; *, $p < 0.02$, *versus* vehicle-basal condition.

and shipment, latrunculin pretreatment and stimulation time was limited to 1 h rather than the 2-h period used with mouse islets, which cumulatively resulted in a lesser yet still significant secretory response to glucose stimulation (Fig. 1*B*). Importantly, each batch of human islets showed the latrunculin-potentiated effect upon glucose-stimulated insulin release, whereas basal secretion was comparable to the vehicle (DMSO)-treated islets (Fig. 1*B*). Because islets contain multiple cell types, 70–80% of which are insulin-containing beta cells, cultured MIN6 beta cells were used to further confirm that this potentiating effect of latrunculin was transduced through the beta cells and not one of the other islet cell types. This potentiating effect occurred very rapidly and was evident within 5 min of stimulation with glucose (Fig. 1*C*). Latrunculin also potentiated insulin release from MIN6 cells in response to KCl and phorbol 12-myristate 13-acetate (PMA) as well as calcium-stimulated secretion from streptolysin-O-permeabilized cells (21). Moreover, the actin-depolymerizing effect of latrunculin was validated by analysis of the F:G-actin ratio, converting the F-actin: G-actin ratio from ~20:80% in unstimulated or vehicle-treated cells to ~1:99% (data not shown). Thus the potentiating effect of latrunculin was found to be conserved across species and relevant to human islet function. Moreover, the MIN6 beta cell line was found to be an appropriate model system in which to pursue a mechanistic study of the role of F-actin in beta cell secretion.

To determine how latrunculin facilitated this potentiation, insulin granule localization was examined. Electron micrograph images of latrunculin-treated MIN6 cells showed the prevalence of granules localized at the plasma membrane (Fig. 2*A*, *right panel*). In 10 images of latrunculin-treated cells collected, more than 90% exhibited this phenotype. In contrast, vehicle-treated cells contained only a few granules at the cell periphery (Fig. 2*A*, *left panel*; *arrow* denotes plasma membrane between neighboring cells) in all fields. Insulin immunofluorescent confocal microscopy of vehicle- or latrunculin-treated MIN6 cells confirmed the identity of the granules localized at the PM as insulin-containing (Fig. 2*B*). Punctate insulin staining was visible broadly across the expanse of the beta cells under basal conditions, with regrouping of granules closer to the cell periphery after only 5 min of glucose stimulation. Latrunculin treatment mimicked this glucose-induced redistribution of granules to the cell periphery but did so in the absence of glucose. Immunofluorescent images of more than 30 clusters of latrunculin-treated cells showed the phenotype in Fig. 2*B*. In a third approach, subcellular fractions were prepared from MIN6 cells treated with vehicle or latrunculin to quantify the extent of the granule redistribution induced by latrunculin. The fractionation procedure was validated in two ways: 1) demonstration of the highest insulin content in the insulin SG fraction with lesser but significant levels in the PM fraction and none in the cytosolic fraction (28, 32, 33); 2) the presence of marker

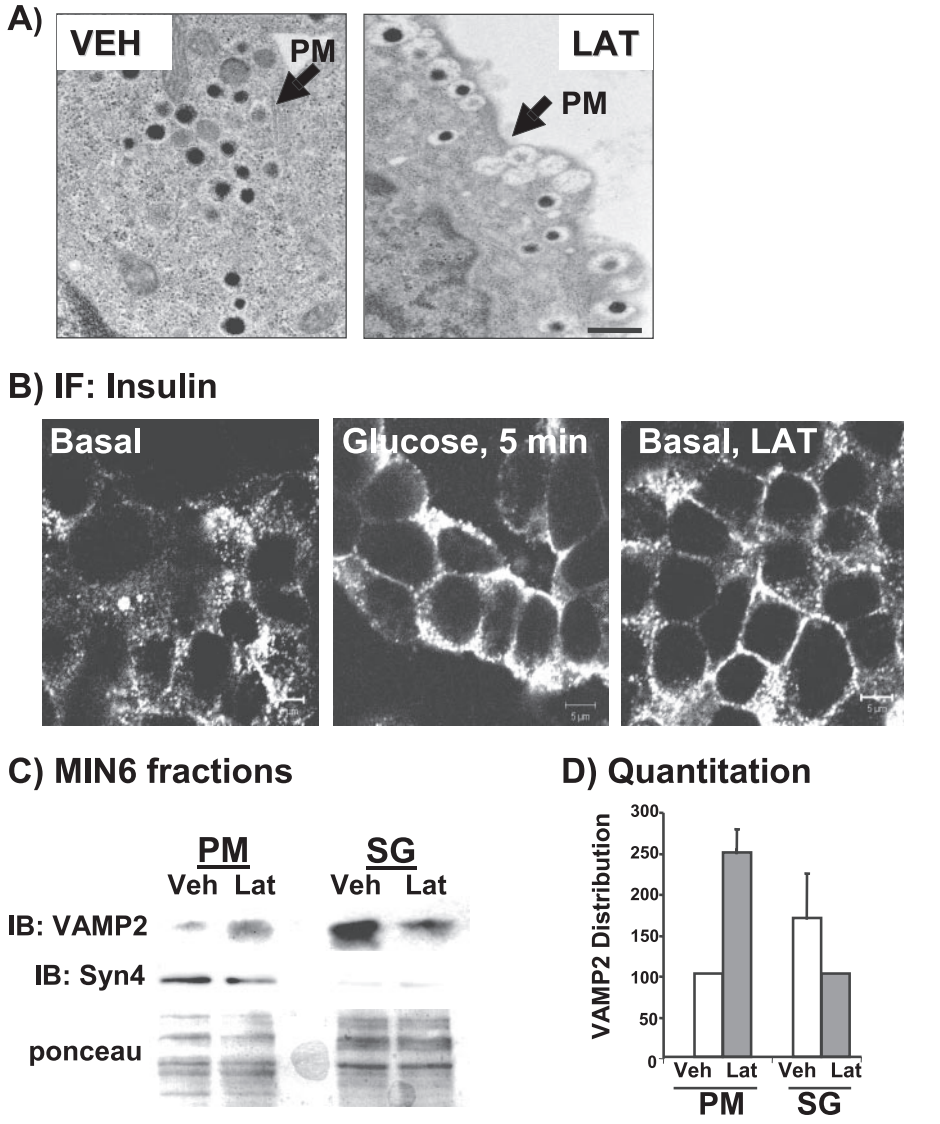

FIGURE 2. **Latrunculin causes increased granule accumulation at the plasma membrane in the absence of glucose.** *A*, transmission electron microscopy of MIN6 cells treated with vehicle (*VEH*) or latrunculin (*LAT*). *Bar* = 500 nm. *B*, latrunculin treatment mobilizes granules toward the plasma membrane compartment from the storage granule pool under basal conditions. MIN6 cells were left unstimulated, stimulated with 20 mM glucose for 5 min, or treated with 10 μM latrunculin for 2 h and then fixed and permeabilized for anti-insulin immunofluorescent (*IF*) confocal microscopy. *Bar* = 5 μm. *C*, MIN6 cells were treated with latrunculin or the DMSO vehicle for 2 h and then subfractionated, and 20 μg of protein from the PM and SG fractions were resolved on 12% SDS-PAGE for immunoblotting. Ponceau S staining was used to verify equal loading; syntaxin immunoblotting (*IB*) was used to validate PM fraction integrity in each fractionation. Data are representative of two independent experiments. *D*, optical density scanning quantitation (each set of fractions normalized to VEH control = 100%) of VAMP2; data shown are the average ± S.E. of three independent sets of fractions. Ponceau S staining was used to verify loading in SG and PM fractions each experiment.

proteins in the PM (Syntaxin 4, Syntaxin 1A), the SG (VAMP2, phogrin), and the Cyto fractions (Cdc42, Munc18c). In three independent sets of fractions, latrunculin induced an ~2.5-fold increase in VAMP2-bound insulin granules localized to the PM, with a coordinate ~40% loss from the SG pool (Fig. 2, *C* and *D*). Ponceau S staining was used to validate equal loading in each experiment. Thus, latrunculin-induced F-actin depolymerization allowed a flow of insulin granules to the PM in the absence of the glucose stimulus.

Glucose-induced Dissociation of F-actin from Syntaxin 4—We have previously reported that F-actin is dynamically reorganized in response to glucose stimulation in islet beta cells, a phenomenon that is coupled to Syntaxin 1 association (20, 21). F-actin associated in a specific manner, as IgG alone or voltage-dependent calcium channel (VDCC) primary antibodies failed to co-immunoprecipitate F-actin. These studies also showed that Syntaxin 1 associates only with F-actin and not G-actin; treatment of cells with actin depolymerizing agents destroyed this association. We have since demonstrated a requirement for a second syntaxin isoform in insulin granule exocytosis, Syntaxin 4 (25). Here we show that like Syntaxin 1, Syntaxin 4 associated with F-actin under basal conditions (Fig. 3, *A* and *B*). Also similar is the marked significant reduction of actin association with Syntaxin 4 after 10 min of glucose stimulation. Following 30 min of glucose stimulation actin reassociated with Syntaxin 4, albeit to a lesser extent than it did with Syntaxin 1. Treatment of cells with latrunculin abolished ~90% of actin interaction with Syntaxin 4 (Fig. 3*C*), indicating that it was F-actin and not G-actin that interacted with Syntaxin 4. These data expand upon the current notion of F-actin serving as a barrier by suggesting that the negative function of F-actin is mediated through its association with multiple plasma membrane-bound syntaxins.

F-actin Directly Associates with Only the Syntaxin 4 Isoform—To determine how the SNARE proteins might confer interaction with F-actin, sequence analyses of v- and t-SNARE proteins for potential homology with any known actin-binding protein motifs were conducted. Although no homologies were identified in VAMP2, SNAP-25, or Syntaxin 1A, Syntaxin 4 was found to have some homology to a motif known as "spectrin-like." To determine whether Syntaxin 4 might bind in a direct manner to F-actin, an *in vitro* actin sedimentation/spin-down assay was employed. Recombinant soluble forms of each SNARE protein (transmembrane domain deleted), expressed in *E. coli* and purified, were incubated with F-actin in a calcium-containing binding buffer and subsequently centrifuged to pellet F-actin and associated proteins. Proteins in each fraction were resolved on SDS-PAGE for detection by Coomassie Blue staining. The known F-actin-binding protein, α-actinin,

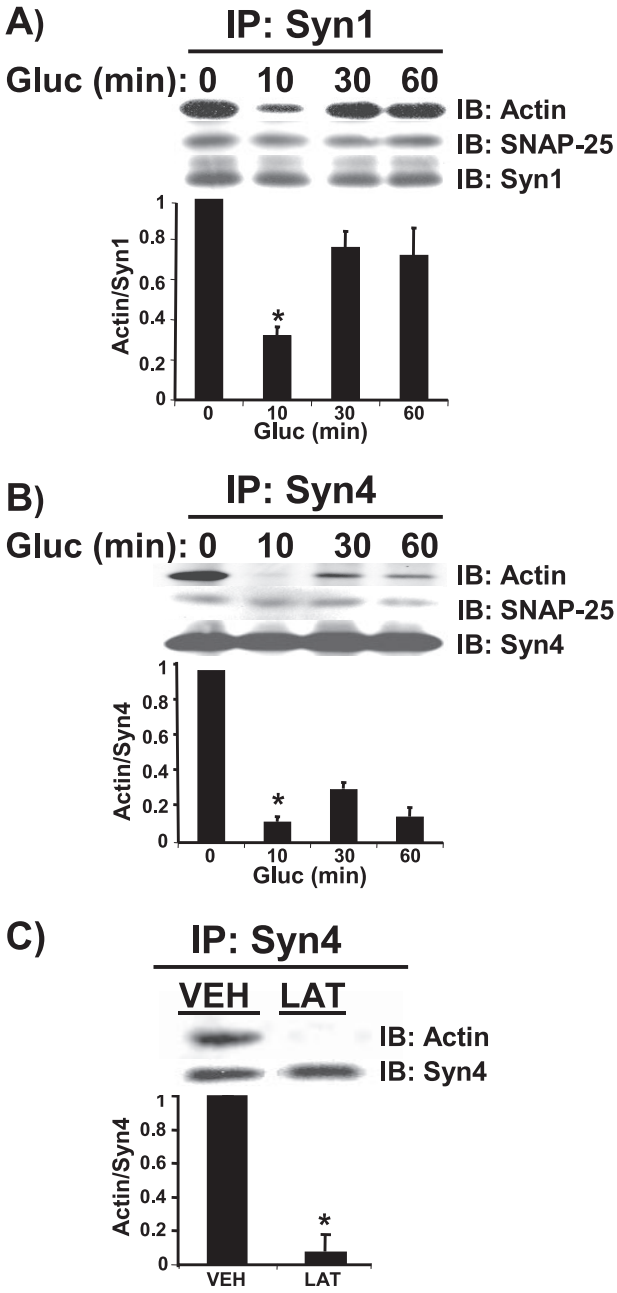

FIGURE 3. **Glucose-induced dissociation of F-actin from Syntaxin 1A and Syntaxin 4.** MIN6 cells were preincubated in MKRBB for 2 h and stimulated with 20 mM glucose (*Gluc*) for 10, 30, and 60 min. Detergent cell lysates were prepared by harvesting in lysis buffer containing 1% Nonidet P-40 and *n*-octylglucoside. Cleared detergent cell lysates (2 mg of protein) were immunoprecipitated (*IP*) with mouse anti-Syntaxin 1 (*A*) or rabbit anti-Syntaxin 4 (*B*) for 2 h at 4 °C. Immunoprecipitates were resolved on 12% SDS-PAGE, and proteins were transferred to PVDF for immunoblotting (*IB*) with mouse anti-Syntaxin 1A or Syntaxin 4, anti-SNAP-25, and rabbit anti-actin. *C*, lysates prepared from cells pretreated for 2 h with vehicle (DMSO, *VEH*) or latrunculin (*LAT*) were used in immunoprecipitation reactions with anti-Syn4 antibody for subsequent immunoblotting for co-immunoprecipitation of actin. Parallel reactions including IgG immunoprecipitation reactions were included to control for nonspecific binding as demonstrated previously (Ref. 21; not shown here). Data are representative of at least five independent co-immunoprecipitation experiments. Optical density scanning quantitation of actin association with syntaxin is shown directly *below* each of the three immunoprecipitation studies (each set of lysates normalized to basal = 1). *Bars* represent the average ± S.E. of 3–5 independent experiments.

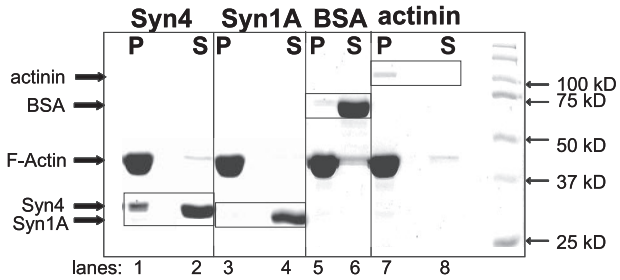

FIGURE 4. **Syntaxin 4 but not Syntaxin 1A binds directly to F-actin *in vitro*.** Recombinant purified proteins were tested for direct F-actin binding in an *in vitro* sedimentation assay. Following incubation and centrifugation, F-actin and associated binding proteins are recovered in the pellet (*P*) fraction, and non-F-actin-binding proteins remain in the supernatant (*S*). Proteins were resolved on 10% SDS-PAGE and detected by Coomassie Blue staining. This reaction was determined to be at saturation for binding (data not shown). Data are representative of six independent experiments using four different preparations of proteins.

appropriately localized to the pellet (*P*) with F-actin (Fig. 4, *lanes 7* and *8*), whereas BSA served as the negative control in this assay and localized to the supernatant (*S*) (Fig. 4, *lanes 5* and *6*). Recombinant Syntaxin 1A also remained strictly in the supernatant (Fig. 4, *lane 4*), as did VAMP2 (data not shown). Remarkably, Syntaxin 4 protein was present in both the pellet and supernatant fractions (Fig. 4, *lanes 1* and *2*). Dosage studies with increasing amounts of Syntaxin 4 protein input indicated this to be a dose-dependent association reaching saturation, where as much as ~25% of the Syntaxin 4 protein input pelleted with F-actin (data not shown). These data indicated that Syntaxin 4 had the ability to interact directly with F-actin, whereas Syntaxin 1A associated exclusively via an indirect mechanism.

To determine which region of Syntaxin 4 conferred direct interaction with F-actin, a series of C- and N-terminal truncations (Fig. 5*A*) were made in the context of GST-Syntaxin 4 (ΔTM, soluble form). Coomassie Blue staining showed that all GST-Syntaxin 4 truncation proteins migrated at the correct molecular weight and as single bands (Fig. 5*B*). GST was cleaved, and the remaining Syntaxin 4 fragments were purified for use in the F-actin spin-down assay. In each assay, recombinant Syntaxin 1A and Syntaxin 4 were used as negative and positive controls for F-actin interaction, respectively (data not shown). C-terminal deletion of domains H3, Hc, or the N-terminal deletion of residues 1–38 failed to abolish Syntaxin 4 interaction with F-actin (Fig. 5*C*). Further delineation of the binding region was detected by immunoblotting instead of Coomassie Blue, given the small molecular weight of the protein. This served as a means to enhance detection of any interaction, taking advantage of the N-terminal epitope recognized by this particular antibody (epitope is residues 2–23 of Syntaxin 4). Using this method, it was seen that the C-terminal deletion up through the Hb domain did ablate binding to F-actin (Fig. 5*D*). Subsequent truncations of the Ha and Hb domains in the context of the full soluble Syntaxin 4 protein were constructed to determine further the importance of the Ha and Hb domains individually but, unfortunately, were labile upon cleavage from the GST protein. Because these binding data delineated the N-terminal Ha-Hb region, comprising residues 39–112, as the minimal region sufficient to confer binding of Syntaxin 4

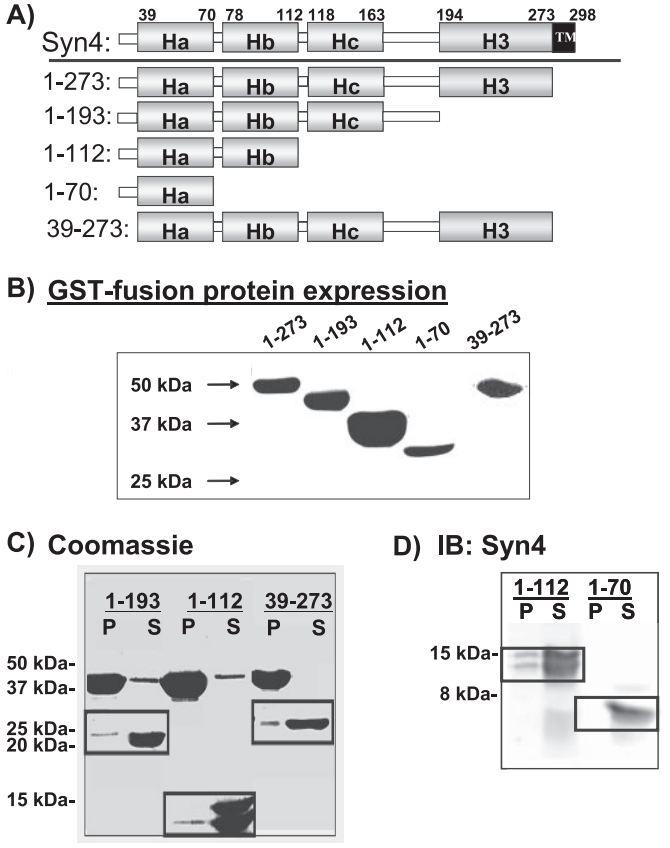

FIGURE 5. **The region containing the HA-HB domains of Syntaxin 4 is necessary and sufficient to confer direct binding to F-actin.** *A*, four C-terminal truncations and one N-terminal truncation of Syntaxin 4 were generated as GST fusion proteins for expression in *E. coli* and purification on glutathione-Sepharose. *B*, Coomassie Blue staining showed the expression of GST fusion Syntaxin 4 truncation proteins. *C*, thrombin-cleaved Syntaxin 4 N-terminal and C-terminal truncated fragments 1–194, 1–112, and 39–273 were prepared at a concentration of 1 mg/ml for use in the *in vitro* actin sedimentation assay. Both the supernatants (*S*) and pellets (*P*) were subjected to 15% SDS-PAGE for Coomassie Blue staining. Syn4 and Syn1A reactions were used as positive and negative controls, respectively, in each experiment (see Fig. 4). *D*, purified Syntaxin 4 C-terminal truncations 1–112 and 1–70 were prepared and tested in the actin sedimentation assay. Both the supernatants and the pellets were subjected to 18% SDS-PAGE followed by transfer to PVDF membranes for immunoblotting with rabbit anti-Syntaxin 4. Data are representative of 2–3 independent sets of proteins.

with F-actin, GST-(39–112) was constructed, but it also was labile *in vitro*. The importance of these far N-terminal residues in Syntaxin 4 structure has been reported and likely explains the instability of our constructs lacking this region (34). Thus, the *in vitro* assay data suggested the F-actin interacting region of Syntaxin 4 to be between amino acids 39–112. Notably, this region also contains the predicted spectrin-like motif.

Selective Separation of Syntaxin 4 from F-actin Enhances Granule Mobilization and Exocytosis—To determine the requirement for Syntaxin 4 binding to F-actin in cells, the Syntaxin 4 actin-binding region (residues 39–112) was used as a selective competitive inhibitor. This small region was fused to the C terminus of the EGFP as shown in Fig. 6*A*, which enabled visualization of its localization within transfected cells and easier detection of its expression by immunodetection on SDS-PAGE (Fig. 6*B*, *IB:EGFP* in lysate). Plasmids encoding EGFP-

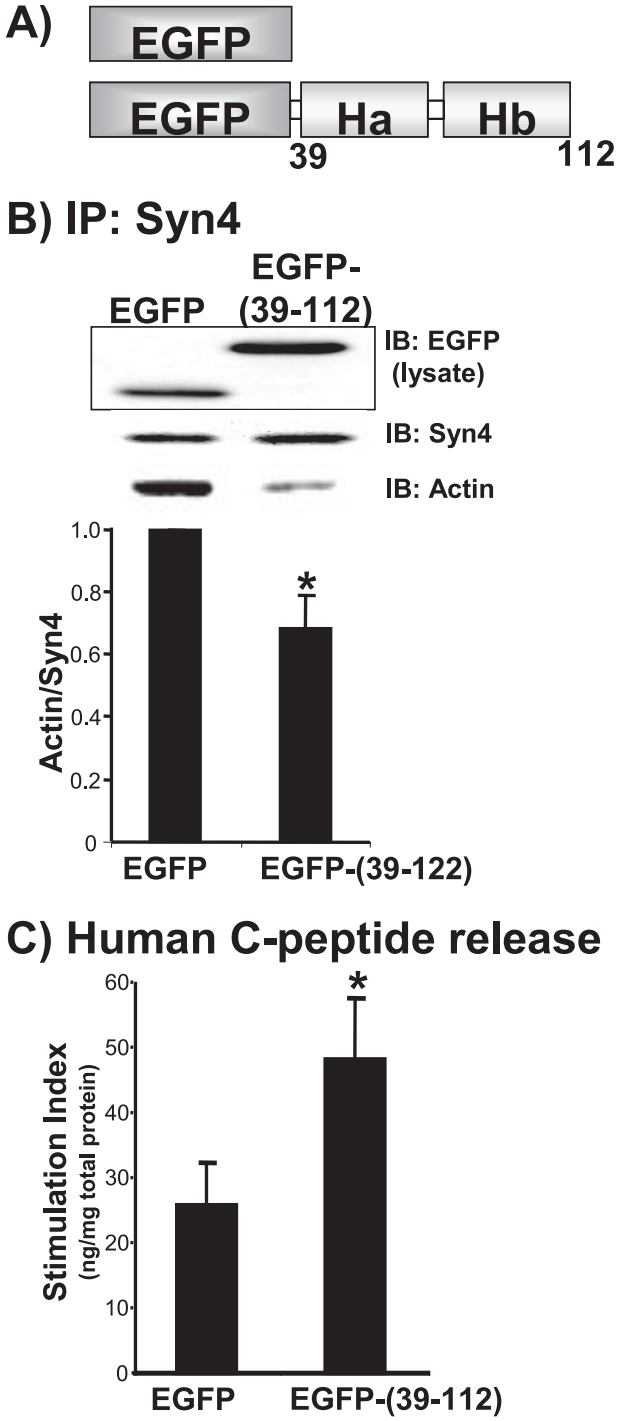

FIGURE 6. **Expression of Syntaxin 4 residues 39–112 in MIN6 cells disrupted the endogenous F-actin-Syn4 association and increased glucose-stimulated secretion.** *A*, the Ha-Hb region of Syntaxin 4 was fused to the C terminus of EGFP for expression in mammalian cells. This is a schematic representation of EGFP and EGFP-(39–112) proteins. *B*, MIN6 lysates expressing the ~37-kDa EGFP-(39–112) protein were used for immunoprecipitation (*IP*) with Syntaxin 4 antibody and immunoblotted (*IB*) for co-precipitation of actin. EGFP (29 kDa) in lysates served as control; the actin/Syn4 ratio in EGFP-expressing lysates was set equal to 1 for normalization in each of four immunoprecipitation experiments (*, $p < 0.05$). *C*, MIN6 cells were co-transfected with EGFP or EGFP-(39–112) with human proinsulin to report effects upon glucose-stimulated human C-peptide secretion only from transfected cells. MIN6 cells were preincubated in glucose-free MKRBB followed by stimulation with 20 mM glucose for 30 min. Data represent the mean ± S.E. from five independent experiments normalized for total protein content. Data were normalized to the unstimulated level for each construct to obtain stimulation index (*, $p < 0.05$).

(39–112) or EGFP vector alone were transfected into MIN6 cells and effect upon Syntaxin 4-F-actin association evaluated by immunoprecipitation with anti-Syntaxin 4 antibody and actin immunoblotting. Because the EGFP-(39–112) fragment did not contain the epitope recognized by the Syntaxin 4 antibody, only endogenous Syntaxin 4 was immunoprecipitated. Indeed, expression of the EGFP-(39–112) resulted in an ~30% decrease in co-precipitation of endogenous Syntaxin 4-F-actin complexes. EGFP-(39–112) action was not due to inadvertent binding to other Syntaxin 4 binding partners, because immunoprecipitation of this fusion protein failed to co-precipitate proteins such as Syntaxin 4, VAMP2, SNAP-25, and Munc18c (data not shown). The analogous region of Syn1A was not used for comparison, as this region of Syntaxin 1A is known to interact directly with another important exocytotic protein, Munc13-1 (35). Despite its ability to dissociate endogenous F-actin-Syntaxin 4 complexes and to bind to F-actin *in vitro*, stable association of the peptide with endogenous F-actin could not be detected consistently (data not shown). Although EGFP-(39–112) protein expression levels were substantial, conformational changes in peptide structure due to its fusion to EGFP may have impaired its ability to stably interact with F-actin. Unlike latrunculin treatment, the EGFP-(39–112) expression had no effect upon global cellular F-actin content (F:G-actin ratio was ~25:75%), such that the action of the inhibitory peptide was more likely through selective separation of F-actin from Syntaxin 4 and not via dispersal of the cortical F-actin network to allow granules to gain access to the plasma membrane.

The EGFP-(39–112) competitive inhibitory fragment was then used to evaluate the functional importance of the endogenous Syntaxin 4-F-actin association in glucose-stimulated insulin secretion. Because transfection efficiency was ~50%, the human C-peptide reporter assay was utilized as a means of measuring secretion only from transfectable cells. MIN6 cells were co-transfected with EGFP-(39–112) or vector control together with human proinsulin cDNA. Human C-peptide (derived from human proinsulin) is synthesized and packaged in an identical fashion to mouse C-peptide and insulin in granules but is immunologically distinct from mouse C-peptide and serves as a reporter of secretion from transfectable cells. MIN6 cells transfected with EGFP vector responded to glucose stimulation by eliciting a 26% increase in insulin release (Fig. 6*C*), similar to levels reported by others using this particular reporter assay (36, 37). However, expression of EGFP-(39–112) increased insulin release to ~49%, suggesting that the selective disruption of F-actin binding to Syntaxin 4 enhanced insulin exocytosis. Thus, the potentiating effect of latrunculin could be recapitulated, at least in part, by competitive inhibition of F-actin binding to Syntaxin 4.

Disruption of F-actin Binding to Syntaxin 4 Enhances Granule Mobilization and Syntaxin 4 Accessibility—Given the functional parallels between actions of EGFP-(39–112) with latrunculin upon insulin secretion, we next sought to determine if the EGFP-(39–112) inhibitor impacted granule localization. MIN6 cells expressing either EGFP of EGFP-(39–112) were subfractionated, and VAMP2 accumulation in PM and SG fractions was assessed. Fig. 7 shows a ~1.6-fold increase in VAMP2 in the PM fraction of EGFP-(39–112)-expressing cells compared with cells expressing EGFP alone ($p < 0.0002$). This increase occurred under basal conditions, similar to that with latrunculin treatment. This corresponded to a ~30% decrease of VAMP2 from the SG fraction of EGFP-(39–112) cells relative to control ($p < 0.0001$). These data indicate that VAMP2-bound granules were inappropriately mobilized to the PM in the absence of the glucose stimulus.

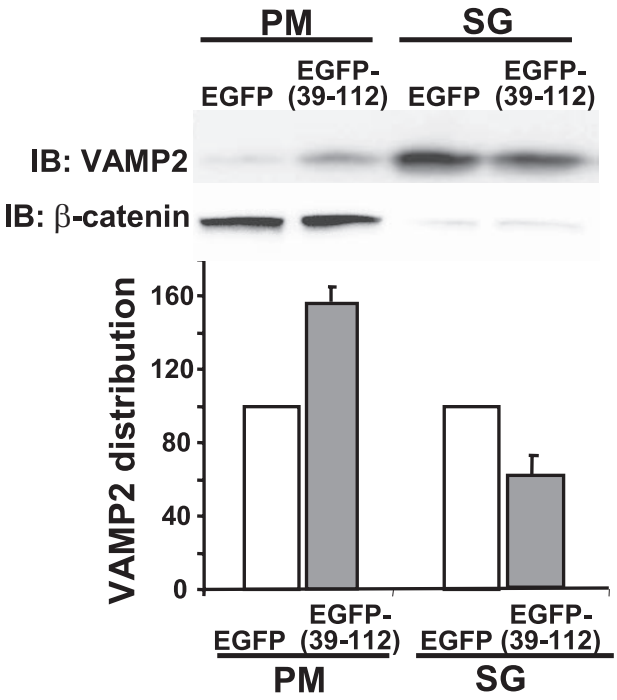

FIGURE 7. **Like latrunculin treatment, expression of EGFP-(39–112) mobilizes granules into the PM compartment from the storage granule pool under basal conditions.** MIN6 cells were transfected with EGFP or EGFP-(39–112) DNA and 48 h later were subfractionated, and 20 μg of protein each from the PM and SG fractions was resolved on 12% SDS-PAGE for immunoblotting (*IB*). Optical density scanning quantitation (each set of fractions normalized to EGFP control = 100%) of VAMP2. Data are shown as the average ± S.E. of four independent sets of fractions. β-Catenin immunodetection was used to verify PM fraction integrity and equal protein loading in each set of PM fractions; Ponceau S staining was used to verify loading in SG and PM fractions in each experiment.

In addition to increasing granule number at the PM, we speculated that the role of F-actin binding to Syntaxin 4 might be to negatively regulate Syntaxin 4 accessibility by VAMP2. To test this possibility, exogenous GST-VAMP2 (soluble form, ΔTM) protein linked to Sepharose beads was added to cell lysates to "probe" for accessible Syntaxin 4, *i.e.* Syntaxin 4 available for binding. From unstimulated MIN6 cells left untreated or treated with vehicle (DMSO), the GST-VAMP2 was able to co-precipitate Syntaxin 4 protein (Fig. 8*A*, *lane 1*). Interestingly however, GST-VAMP2 co-precipitated significantly more Syntaxin 4 protein (2.4 ± 0.2, $p < 0.0005$) from lysates prepared from latrunculin-treated cells (Fig. 8*A*, *lane 2*).

However, even though latrunculin-induced F-actin depolymerization rendered Syntaxin 4 more accessible to VAMP2 and also significantly increased the number of granules juxtaposed to the PM under basal conditions, the amount of endogenous VAMP2 co-immunoprecipitated with Syntaxin 4 was not coordinately increased in latrunculin-treated lysates when com-

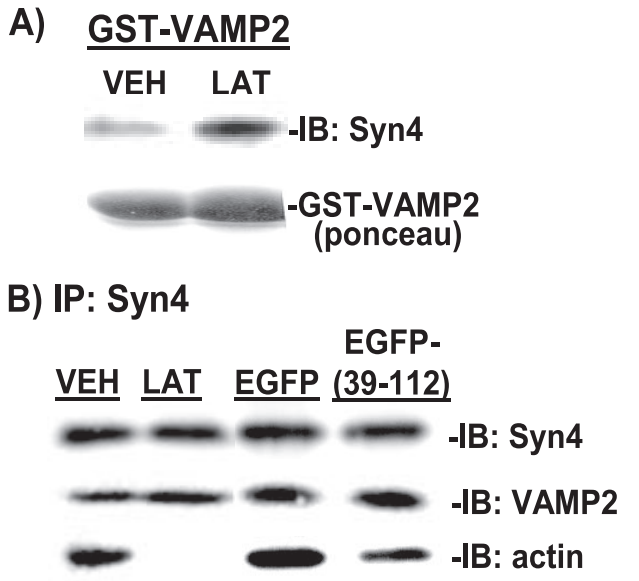

FIGURE 8. **EGFP-Syntaxin4 (39–112) expression increases Syntaxin 4 accessibility but not VAMP2 docking/fusion at Syntaxin 4 sites.** *A*, MIN6 cells were treated with vehicle (*VEH*) or latrunculin (*LAT*) for 2 h in glucose-free MKRBB for preparation of cleared detergent lysates for use in GST-VAMP2 (soluble form) interaction assays. Lysate protein (2–3 mg) was combined with GST-VAMP2 linked to beads, and precipitated proteins were resolved on 10% SDS-PAGE for Syntaxin 4 immunoblotting (*IB*). Data are representative of four independent sets of cell lysates. *B*, MIN6 cells were left untransfected or were transfected with pEGFP or pEGFP-(39–112) DNA. Forty-eight h later, cells were preincubated in glucose-free MKRBB with or without DMSO or LAT added for 2 h and harvested for preparation of cleared detergent lysates. Lysate protein (2 mg/reaction) was incubated with anti-Syntaxin 4, and co-immunoprecipitated proteins (*IP*) were resolved on 12% SDS-PAGE for immunoblotting with anti-Syntaxin 4, anti-VAMP2, and anti-actin antibodies. Data are representative of 3–6 independent experiments.

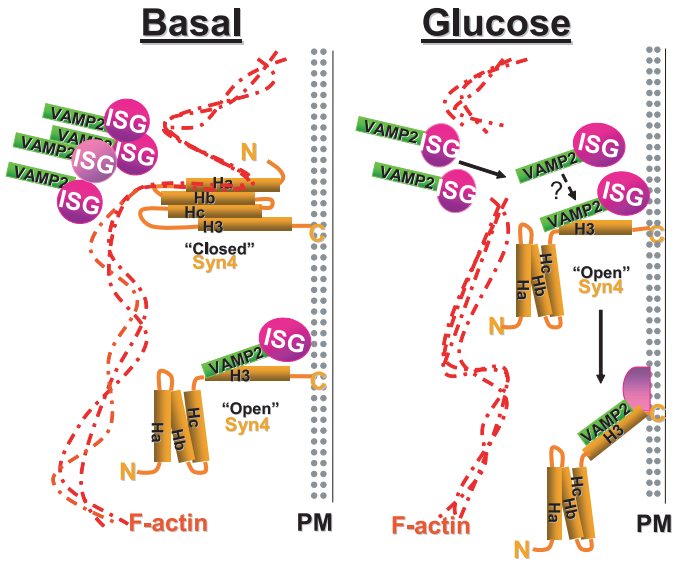

FIGURE 9. **Model depicting potential mechanism of regulation of insulin exocytosis by F-actin-Syntaxin 4 complexes under basal and glucose-stimulated conditions.** *Left panel*, under basal conditions, F-actin binds to residues 39–112 of Syntaxin 4 (Ha-Hb domains), decreasing Syntaxin 4 accessibility to VAMP2 (consistent with Syntaxin 4 being in the *closed* conformation) and also restricting the flow of storage pool granules into the readily releasable pool at the plasma membrane. However, some Syntaxin 4 sites are occupied by granules, consistent with the requirement for Syntaxin 4 in first-phase insulin release (25). *Right panel*, glucose stimulation results in the localized reorganization of actin, which allows the storage pool of insulin granules to traffic to the plasma membrane and increases accessibility of VAMP2 to Syntaxin 4 sites (*open* conformation) to facilitate granule fusion and insulin release. An additional step triggered by glucose to "activate" VAMP2 docking is suggested (see *question mark*).

pared with vehicle-treated lysates (Fig. 8*B*, *lanes 1* and *2*). These data suggest that the mechanism is more complex than can be explained by a simple inverse relationship between loss of F-actin binding corresponding to increased VAMP2 binding. In addition, Syntaxin 4-VAMP2 association was similar between EGFP-(39–112) and EGFP-expressing cell lysates (Fig. 8*B*, lanes 3–4), even though F-actin binding to Syntaxin 4 was significantly reduced by expression of EGFP-(39–112). Co-immunoprecipitation experiments were also conducted using PM fractions in place of whole cell lysates and similarly showed no increased association of VAMP2 with latrunculin treatment of EGFP-(39–112) expression (data not shown). This lack of impact upon VAMP2-Syntaxin 4 association correlates with the lack of effect of latrunculin or the EGFP-(39–112) fragment upon basal insulin release. Thus, these data suggest that F-actin negatively regulates exocytosis via binding and blocking Syntaxin 4 accessibility but also reveal the necessity for additional signals and/or steps required to trigger vesicle docking and fusion.

DISCUSSION

The importance of F-actin in insulin exocytosis has long been debated, yet its relevance to human insulin release has remained unknown. Here we demonstrate for the first time that the potentiating effect of F-actin depolymerization upon glucose-stimulated insulin secretion is a conserved and valid mechanism in human islets. Validation of this relevance prompted us to investigate the mechanism by which F-actin functioned in insulin exocytosis, and we show here that this selectively involves Syntaxin 4. Syntaxin 4 was found to function as a novel actin-binding protein, associating with F-actin via its N-terminal region containing the Ha-Hb domains. This association was specific for Syntaxin 4, as Syntaxin 1A failed to directly bind to F-actin. This represents the first mechanistic evidence in support of functionally distinct roles for these seemingly redundant syntaxin isoforms in insulin granule exocytosis.

Our data show that these Syntaxin 4-F-actin complexes were key to the mechanism by which F-actin regulates granule flow/mobilization. One possible role for this complex might be that Syntaxin 4 serves as an attachment site of F-actin to the plasma membrane, such that under basal conditions Syntaxin 4 might exist in two conformations (see model, Fig. 9 *left panel*): 1) "closed" and bound by F-actin to block granule docking, consistent with data presented here showing that Syntaxin 4 was more accessible in cells treated with latrunculin; and 2) "open" and bound by a granule to support first-phase insulin release. Then upon glucose-stimulated actin reorganization (Fig. 9, *right panel*), granules mobilize and may preferentially dock at open Syntaxin 4 sites for subsequent fusion and insulin release. The novel F-actin binding motif of Syntaxin 4 functioned as a competitive inhibitor of the direct association between F-actin-Syntaxin 4, mimicking actions of latrunculin but without inducing global changes in cellular F-actin content. This suggests that it may be through this particular interaction with

Syntaxin 4 that F-actin exerts some of its "barrier" function in exocytosis. Whether this association also plays a role in the "positive" role for F-actin in granule mobilization remains untested. To date there is evidence to suggest that the positive role is mediated by vesicle-microfilament interactions (38–41).

Interestingly, however, VAMP2 association with syntaxin was not increased upon release of F-actin binding from Syntaxin 4. This could be due to a requirement for an additional stimulus-dependent/induced step(s) that precedes the docking and fusion steps in exocytosis. It is known that VAMP2-Syntaxin binding occurs more efficiently in cells than *in vitro*, and this has been proposed to be due to a requirement for VAMP2 activation, Syntaxin accessibility, or both (42). Thus, perhaps the reason docking/fusion was not enhanced under conditions where Syntaxin 4 accessibility and granule mobilization to the PM were both increased was because of a missing cellular signal triggered by glucose required for VAMP2 activation. The small Rho-family GTPase Cdc42 has been suggested as a possible candidate (42) based upon data showing: 1) Cdc42 binds directly to the N-terminal 28 residues of the VAMP2 protein on the insulin granule (28); 2) Cdc42 activation correlates with mobilization of VAMP2-bound granules to the PM, specifically in response to stimulation with glucose and not KCl (28, 43); 3) deregulation of Cdc42 activation via depletion of its GDI results in inappropriate fusion and release of insulin in the absence of the glucose stimulus (44); and 4) Cdc42 is required exclusively for the second phase/mobilization phase of insulin secretion from islets (43). This would be a glucose-specific signal independent of the calcium signal that is thought to couple the calcium-sensitive complexin protein in mediating Syntaxin 1A-dependent exocytosis in neurotransmitter release (45). However, the specifics as to how glucose Cdc42 might activate VAMP2 to promote granule targeting to particular syntaxin-based active sites to facilitate second-phase secretion are unclear because the characterization of such active sites remains incomplete.

Our finding that Syntaxin 4 in particular associated directly with F-actin represents a step toward distinguishing the functions of Syntaxin 4 from Syntaxin 1A and in characterizing the active site used for second-phase secretion. Syntaxin 4 binding to F-actin was mediated via its N-terminal Ha-Hb region and not through its H3/SNARE domain, consistent with alignments showing lesser conservation in the N terminus of these Syntaxin isoforms 35% identical in Ha and 38% in Hb *versus* 56% in H3 domain). Moreover, VAMP2 contains the conserved SNARE domain and failed to bind. Only very recently has another SNARE protein been reported to directly interact with actin, the R-SNARE protein Ykt6p, although the binding motif remains to be identified (46). A second distinguishing characteristic was the slow and incomplete reassociation of F-actin with Syntaxin 4 after the initial glucose-induced disruption of binding in the co-immunoprecipitation studies relative to the kinetics of F-actin and Syntaxin 1A association. These kinetic differences are consistent with the notion that Syntaxin 4 docking sites are accessible and operative during second-phase secretion, although this concept awaits further examination using primary beta cells.

Differential localization to caveolae may also mark distinct syntaxin-based active sites. Data from multiple studies in divergent cell types show that Syntaxin 1A is clustered into "active sites" by caveolae (47–49). A recent study used stimulated emission depletion (STED) microscopy to show that the SNARE motifs of Syntaxins 1 and 4 mediate specific syntaxin clustering by homo-oligomerization, thereby spatially separating sites for different biological activities (50). Moreover, caveolar clustering can be induced by localized F-actin depolymerization (51). Furthermore, L-type calcium channels have been localized in or nearby caveolae (52), and overexpression studies performed in cultured beta cells showed that increased Syntaxin 1A protein inhibits L-type calcium channel activity, whereas overexpression of Syntaxin 4 is without effect (53).

The Syntaxin 4 fragment comprising the Ha-Hb domain markedly increased granule flow to the PM, mimicking the effects induced by latrunculin in unstimulated cells, as well as the effect of acute glucose stimulation (28). Like glucose stimulation, the 39–112 inhibitory fragment did not cause global changes in F-actin content, whereas latrunculin is a global actin depolymerizing agent. These data suggest then that Syntaxin 4-F-actin complexes may be a target of glucose-induced localized F-actin reorganization and may be the means by which glucose coordinates the timing of increased Syntaxin 4 accessibility with increased granule accumulation at the plasma membrane. Alternatively, it is possible that this 39–112 fragment interfered with Syntaxin 4 binding to other factors involved in actin remodeling. Of the SNARE and SNARE accessory proteins, only n-Sec1/Munc18 and Munc13 proteins are known to interact with the N-terminal helices of syntaxin proteins (35, 54); but we failed to see any alteration in endogenous Syntaxin 4-Munc18c association in cells expressing the 39–112 fragment, and the Syntaxin 4 isoform has yet to be shown to interact with Munc13. However, Syntaxin 4 has been shown to bind the actin-binding protein α-fodrin directly (55), and in 3T3L1 adipocytes the Syntaxin 4-fodrin complex is functionally important in insulin-stimulated GLUT4 translocation (56). In addition, the F-actin-severing proteins such as gelsolin and scinderin have been shown to be important in stimulus-secretion coupling in cultured beta cells (22, 57), although neither has been shown to associate with syntaxins.

In summary, these studies provide data to support a new model whereby the negative barrier function of cortical F-actin is mediated in part by a discrete and direct interaction of F-actin with Syntaxin 4 at the plasma membrane and further reveal the existence of a new step in stimulus-induced granule exocytosis that precedes docking. In islet beta cells, this new step requires glucose as the stimulus. Although the Syntaxin 4-F-actin interaction will likely impact exocytosis events in many cells given the ubiquitous expression pattern of these proteins, the kinetics of biphasic insulin release are quite distinct from events such as neurotransmitter secretion or GLUT4 translocation. Second-phase insulin release can occur over a long time period (hours), requiring the readily releasable pool at the plasma membrane to be refilled from the more intracellular storage pool in a carefully metered manner. F-actin is well suited to this task, because release and refill events must occur across the expanses of the cell, yet be coordinated to occur simultaneously to achieve the precisely timed biphasic release of insulin. Future studies will be required to

determine the importance and specific utilization of the Syntaxin 4-F-actin complex in these other cell types.

Acknowledgments—We are grateful to Dr. Chris Newgard and Dr. John Hutton for gifts of the human proinsulin cDNA and MIN6 beta cells, respectively. We thank Raphael Tonade and Erica Daniel for technical assistance with this project. Human islets were obtained through the National Institutes of Health/ICR/ABCC distribution program. Assistance from the Indiana University School of Medicine Electron Microscopy Center was invaluable for these studies.

REFERENCES

1. Barg, S., Eliasson, L., Renstrom, E., and Rorsman, P. (2002) *Diabetes* **51,** Suppl. 1, S74–S82
2. Daniel, S., Noda, M., Straub, S. G., Sharp, G. W., Komatsu, M., Schermerhorn, T., and Aizawa, T. (1999) *Diabetes* **48,** 1686–1690
3. Straub, S. G., Shanmugam, G., and Sharp, G. W. (2004) *Diabetes* **53,** 3179–3183
4. Vikman, J., Ma, X., Hockerman, G. H., Rorsman, P., and Eliasson, L. (2006) *J. Mol. Endocrinol.* **36,** 503–515
5. Lacy, P. E., Howell, S. L., Young, D. A., and Fink, C. J. (1968) *Nature* **219,** 1177–1179
6. Lacy, P. E., Walker, M. M., and Fink, C. J. (1972) *Diabetes* **21,** 987–998
7. Kelly, R. B. (1990) *Cell* **61,** 5–7
8. Malaisse, W. J., Malaisse-Lagae, F., Van Obberghen, E., Somers, G., Devis, G., Ravazzola, M., and Orci, L. (1975) *Ann. N. Y. Acad. Sci.* **253,** 630–652
9. Orci, L., Gabbay, K. H., and Malaisse, W. J. (1972) *Science* **175,** 1128–1130
10. Somers, G., Blondel, B., Orci, L., and Malaisse, W. J. (1979) *Endocrinology* **104,** 255–264
11. Aunis, D., and Bader, M. F. (1988) *J. Exp. Biol.* **139,** 253–266
12. Bader, M. F., Doussau, F., Chasserot-Golaz, S., Vitale, N., and Gasman, S. (2004) *Biochim. Biophys. Acta* **1742,** 37–49
13. Eitzen, G. (2003) *Biochim. Biophys. Acta* **1641,** 175–181
14. Gasman, S., Chasserot-Golaz, S., Malacombe, M., Way, M., and Bader, M. F. (2004) *Mol. Biol. Cell* **15,** 520–531
15. Wang, J. L., Easom, R. A., Hughes, J. H., and McDaniel, M. L. (1990) *Biochem. Biophys. Res. Commun.* **171,** 424–430
16. Howell, S. L., and Tyhurst, M. (1979) *Biochem. J.* **178,** 367–371
17. Howell, S. L., and Tyhurst, M. (1979) *Biochem. J.* **178,** 367–371
18. Snabes, M. C., and Boyd, A. E. (1982) *Biochem. Biophys. Res. Commun.* **104,** 207–211
19. Swanston-Flatt, S. K., Carlsson, L., and Gylfe, E. (1980) *FEBS Lett.* **117,** 299–302
20. Nevins, A. K., and Thurmond, D. C. (2003) *Am. J. Physiol.* **285,** C698–C710
21. Thurmond, D. C., Gonelle-Gispert, C., Furukawa, M., Halban, P. A., and Pessin, J. E. (2003) *Mol. Endocrinol.* **17,** 732–742
22. Tomas, A., Yermen, B., Min, L., Pessin, J. E., and Halban, P. A. (2006) *J. Cell Sci.* **119,** 2156–2167
23. Tsuboi, T., da Silva Xavier, G., Leclerc, I., and Rutter, G. A. (2003) *J. Biol. Chem.* **278,** 52042–52051
24. Ohara-Imaizumi, M., Fujiwara, T., Nakamichi, Y., Okamura, T., Akimoto, Y., Kawai, J., Matsushima, S., Kawakami, H., Watanabe, T., Akagawa, K., and Nagamatsu, S. (2007) *J. Cell Biol.* **177,** 695–705
25. Spurlin, B. A., and Thurmond, D. C. (2006) *Mol. Endocrinol.* **20,** 183–193
26. Low, S. H., Vasanji, A., Nanduri, J., He, M., Sharma, N., Koo, M., Drazba, J., and Weimbs, T. (2006) *Mol. Biol. Cell* **17,** 977–989
27. Beest, M. B., Chapin, S. J., Avrahami, D., and Mostov, K. E. (2005) *Mol. Biol. Cell* **16,** 5784–5792
28. Nevins, A. K., and Thurmond, D. C. (2005) *J. Biol. Chem.* **280,** 1944–1952
29. Lacy, P. E., and Kostianovsky, M. (1967) *Diabetes* **16,** 35–39
30. Spurlin, B. A., Thomas, R. M., Nevins, A. K., Kim, H. J., Noh, H. J., Kim, J. A., Shulman, G. I., and Thurmond, D. C. (2003) *Diabetes* **52,** 1910–1917
31. Ke, B., Oh, E., and Thurmond, D. C. (2007) *J. Biol. Chem.* **282,** 21786–21797
32. Li, G., Kowluru, A., and Metz, S. A. (1996) *Biochem. J.* **316,** 345–351
33. Mitchell, K. J., Tsuboi, T., and Rutter, G. A. (2004) *Diabetes* **53,** 393–400
34. Hu, S. H., Latham, C. F., Gee, C. L., James, D. E., and Martin, J. L. (2007) *Proc. Natl. Acad. Sci. U. S. A.* **104,** 8773–8778
35. Betz, A., Okamoto, M., Benseler, F., and Brose, N. (1997) *J. Biol. Chem.* **272,** 2520–2526
36. Kashima, Y., Miki, T., Shibasaki, T., Ozaki, N., Miyazaki, M., Yano, H., and Seino, S. (2001) *J. Biol. Chem.* **276,** 46046–46053
37. Mulder, H., Lu, D., Finley, J. T., An, J., Cohen, J., Antinozzi, P. A., McGarry, J. D., and Newgard, C. B. (2001) *J. Biol. Chem.* **276,** 6479–6484
38. Varadi, A., Tsuboi, T., and Rutter, G. A. (2005) *Mol. Biol. Cell* **16,** 2670–2680
39. Ivarsson, R., Jing, X., Waselle, L., Regazzi, R., and Renstrom, E. (2005) *Traffic* **6,** 1027–1035
40. Kasai, K., Ohara-Imaizumi, M., Takahashi, N., Mizutani, S., Zhao, S., Kikuta, T., Kasai, H., Nagamatsu, S., Gomi, H., and Izumi, T. (2005) *J. Clin. Investig.* **115,** 388–396
41. Waselle, L., Coppola, T., Fukuda, M., Iezzi, M., El-Amraoui, A., Petit, C., and Regazzi, R. (2003) *Mol. Biol. Cell* **14,** 4103–4113
42. Jahn, R., and Scheller, R. H. (2006) *Nat. Rev. Mol. Cell Biol.* **7,** 631–643
43. Wang, Z., Oh, E., and Thurmond, D. C. (2007) *J. Biol. Chem.* **282,** 9536–9546
44. Nevins, A. K., and Thurmond, D. C. (2006) *J. Biol. Chem.* **281,** 18961–18972
45. Giraudo, C. G., Eng, W. S., Melia, T. J., and Rothman, J. E. (2006) *Science* **313,** 676–680
46. Isgandarova, S., Jones, L., Forsberg, D., Loncar, A., Dawson, J., Tedrick, K., and Eitzen, G. (2007) *J. Biol. Chem.* **282,** 30466–30475
47. Yang, X., Xu, P., Xiao, Y., Xiong, X., Xu, T., Sieber, J. J., Willig, K. I., Heintzmann, R., Hell, S. W., and Lang, T. (2006) *J. Biol. Chem.* **281,** 15457–15463
48. Chamberlain, L. H., Burgoyne, R. D., and Gould, G. W. (2001) *Proc. Natl. Acad. Sci. U. S. A.* **98,** 5619–5624
49. Lang, T., Bruns, D., Wenzel, D., Riedel, D., Holroyd, P., Thiele, C., and Jahn, R. (2001) *EMBO J.* **20,** 2202–2213
50. Sieber, J. J., Willig, K. I., Heintzmann, R., Hell, S. W., and Lang, T. (2006) *Biophys. J.* **90,** 2843–2851
51. Mundy, D. I., Machleidt, T., Ying, Y. S., Anderson, R. G., and Bloom, G. S. (2002) *J. Cell Sci.* **115,** 4327–4339
52. Xia, F., Gao, X., Kwan, E., Lam, P. P., Chan, L., Sy, K., Sheu, L., Wheeler, M. B., Gaisano, H. Y., and Tsushima, R. G. (2004) *J. Biol. Chem.* **279,** 24685–24691
53. Kang, Y., Huang, X., Pasyk, E. A., Ji, J., Holz, G. G., Wheeler, M. B., Tsushima, R. G., and Gaisano, H. Y. (2002) *Diabetologia* **45,** 231–241
54. Fujita, Y., Shirataki, H., Sakisaka, T., Asakura, T., Ohya, T., Kotani, H., Yokoyama, S., Nishioka, H., Matsuura, Y., Mizoguchi, A., Scheller, R. H., and Takai, Y. (1998) *Neuron* **20,** 905–915
55. Nakano, M., Nogami, S., Sato, S., Terano, A., and Shirataki, H. (2001) *Biochem. Biophys. Res. Commun.* **288,** 468–475
56. Liu, L., Jedrychowski, M. P., Gygi, S. P., and Pilch, P. F. (2006) *Mol. Biol. Cell* **17,** 4249–4256
57. Bruun, T. Z., Hoy, M., and Gromada, J. (2000) *Eur. J. Pharmacol.* **403,** 221–224